Equilibrium magnetization in the vicinity of the Bragg glass to vortex glass transition in V_3Si

G. Ravikumar[1] and H. Küpfer[2]
[1]*Technical Physics and Prototype Engineering Division, Bhabha Atomic Research Centre, Mumbai-400085, India*
[2]*Institut für Festkörperphysik, Forschungszentrum Karlsruhe GmbH, D-76021 Karlsruhe, Germany*
(Received 5 May 2005; revised manuscript received 2 August 2005; published 31 October 2005)

We present a study of the quasiequilibrium magnetization of single crystalline V_3Si spheres of different pinning strength in the vicinity of Bragg glass to disordered vortex solid transition. We report a first-order-like magnetization step below the onset of the peak effect. Its occurrence is hysteretic with respect to the direction of field scan. The step is observed only for fields oriented away from the high crystal symmetry directions [110] and [100]. Accompanying the magnetization step is an abrupt reorientation of the vortex lattice towards a crystal symmetry direction. Coupling between the vortex lattice and the underlying crystal lattice is suggested as a possible mechanism for the reorientation transition.

DOI: 10.1103/PhysRevB.72.144530 PACS number(s): 74.25.Qt, 74.25.Ha

I. INTRODUCTION

Competition between elastic intervortex interaction and pinning is responsible for the structural transition of the vortex matter from the quasiordered Bragg glass (BG) to the disordered vortex solid or vortex glass (VG) phase in weakly pinned superconductors.[1] It is identified by a sharp increase in the pinning force and critical current density J_c (peak effect) as a function of field and/or temperature in conventional[2] and high-T_c superconductors.[3] Across the BG-VG transition, nonequilibrium disordered vortex phase can be dynamically introduced at the sample edges[4] and/or at the surface. In addition, within the BG phase region, the nonequilibrium phase can grow by accumulating on the frozen-in disordered phase.[5] Presence of metastable nonequilibrium phases across the peak effect hides the underlying equilibrium state,[6] and therefore thermodynamic nature of this transition is still a matter of debate.

Two experimental procedures were suggested in literature to overcome this problem. (a) Repeated quasistatic field cycling with a small amplitude[6] to suppress the irreversibility due to nonequilibrium phases. Using this procedure, equilibrium magnetization M_{eq} obtained from the minor hysteresis loops exhibits a small step at the onset of the peak effect in $NbSe_2$ (Ref. 6) as well as at the onset of the second magnetization peak in $YBa_2Cu_3O_{7-x}$ (YBCO) (Ref. 7) indicating that the BG-VG transition is a first-order transition. The second procedure (b) is the dynamic equilibration process involving a small ac field applied transverse to the dc field[8,9] which altogether suppresses the irreversibility in magnetization including that arising from the nonequilibrium phases. The quasireversible magnetization thus obtained is reported to exhibit a first-order-like step at the second magnetization peak in $Bi_2Sr_2CaCu_2O_8$ (BSCCO).[9] These experiments clearly establish that the BG-VG transition is a disorder induced melting, which is first order in nature.[9]

The motivation of the present work is to investigate the quasireversible magnetization across the peak effect regime (BG-VG transition) in the conventional superconductor V_3Si obtained by the dynamic equilibration process recently described by us in Ref. 10. The details of this process are somewhat different from that of (b) described above but bears some similarity. We briefly discuss it in the next section. We also studied the dependence of the magnetization on the relative orientation between the field and the crystallographic symmetry axes. The detailed experimental results are presented in Sec. III. Important observations are listed below.

(i) A sharp first-order-like magnetization step in the quasireversible magnetization in both field and temperature scans below the onset of peak effect.

(ii) Occurrence of the step is hysteretic with respect to the direction of the field and temperature scans.

(iii) The magnetization step is observed only for field oriented away from the crystallographic symmetry directions [100] and [110]. It is accompanied by an abrupt change in the orientation of the magnetization with respect to field direction.

It is tempting to associate the first two observations with the BG-VG transition, which is expected to be first order in nature. The third observation may moreover suggest that the flux line lattice (FLL) and the underlying crystal structure hosting the FLL exhibit orientational correlations. In Sec. IV, we discuss a possible mechanism to understand the orientation change of the magnetization.

Borocarbide superconductors[11] and V_3Si (Ref. 12) exhibit structural transition from a low-field triangular to square FLL at higher fields, arising from the coupling between the underlying crystal lattice, which influences the symmetry of the superconducting order parameter, and the FLL. Such a structural transition is explained on the basis of the nonlocal London theory.[11–13] However, to the best of our knowledge the case of FLL oriented away from the symmetry axis is not considered. The third observation suggests that the FLL exhibits a tendency to align with one of the crystal symmetry axes, i.e., a reorientation transition. Analysis of our results indicates that the pinning plays a crucial role in such a transition governed by structural or orientational correlations.

II. EXPERIMENT

Preparation of the single crystalline V_3Si is discussed elsewhere.[14] The crystals were irradiated by fast neutrons of energy more than 1 MeV and fluence of 10^{18} cm^{-2} at 40 °C.

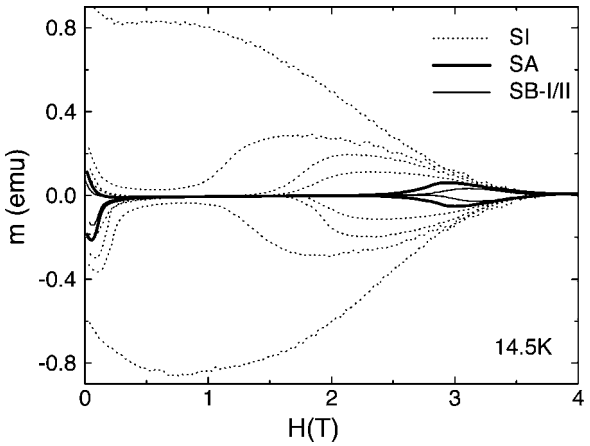

FIG. 1. Magnetization hysteresis loops of the neutron irradiated V_3Si sphere at various stages of annealing are shown in dotted lines. Further two annealing stages give hysteresis loops corresponding to samples SA (thick line) and SB-I/II (thin line).

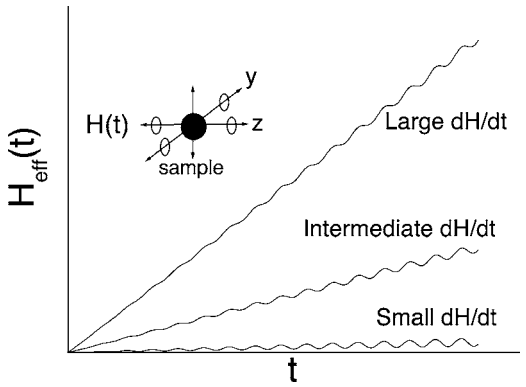

FIG. 2. Field experienced by the sample during a measurement is schematically shown for different field sweep rates. Inset shows the measurement configuration where the sample vibration is transverse to the field direction **z**. Two sets of pick-up coils help in measuring the magnetic moment parallel and perpendicular to the field.

A spherical sample was prepared from this crystal by spark erosion. Subsequent etching and polishing produced a 1.8 mm diameter sphere. Critical temperature of the samples is around 16.1 K. Magnetization of this sample is highly hysteretic without a peak effect indicating strong pinning. When subjected to various thermal annealing steps, the hysteresis progressively decreases producing a pronounced peak effect at higher and higher fields as shown in Fig. 1, indicating the reduction in pinning strength. We used three samples SA (thick line in Fig. 1), SB-I and SB-II in the order of decreasing pinning strength for this study. Most results presented here are obtained on the sample SA. We shall however use the results on SB-I and SB-II to discuss the effect of varying the pinning strength. Spherical sample geometry was chosen in order to obtain uniform demagnetization, to avoid geometrical locking of shielding currents and to reduce disordered phase introduced at the sample edges.

V_3Si exhibits a cubic to tetragonal transition slightly above T_c (Ref. 15) resulting in an anisotropy of about 5% in H_{c2} with maximum along [100] and minimum along [110]. At a given temperature, it implies that pinning is the strongest for $H//[100]$. Accordingly, onset field H_{on} and the peak field H_p in the peak effect region are minimum in this direction. It may further indicate the nonlinear origin of the peak effect phenomenon with respect to the strength of pinning. Other reasons for the strong anisotropy of the BG-VG transition can be the angle dependent coupling energy between crystal lattice and the FLL and the angle dependence in the introduction and/or annealing of frozen disorder.[16]

The [100] direction has been identified and marked in an x-ray goniometer and subsequently placed in the magnetometer. This may result in an error of about 5° in the sample orientations quoted. Magnetization measurements are carried out using a vector vibrating sample magnetometer (VSM) from Oxford Instruments. In the VSM, a superconducting split coil generates a horizontal magnetic field up to 7 T and the sample vibrates transverse to the magnetic field. Two pairs of pick-up coils as shown in the inset of Fig. 2 are used to detect magnetic moment along and perpendicular to the applied field. Magnetic moment is measured by sweeping the dc magnetic field. The linear field sweep rate dH/dt (t is the time variable) is one of the crucial parameters in our experiment. It has been varied from 0.01–0.60 T/min. The other important parameter is the sample vibration amplitude, which can be varied from 0.06 to 1.2 mm. Due to a small field inhomogeneity,[17] the sample effectively sees a longitudinal ac field, which grows with the vibration amplitude and the dc field $H(t)$ varying linearly in time. Typical field $H_{eff}(t)$ experienced by the sample during a measurement involving different sweep rates is schematically depicted in Fig. 2. $H_{eff}(t)$ tends to be monotonic in time for large dH/dt and strongly nonmonotonic for small dH/dt for a given sample vibration amplitude. Conversely, it can be argued that $H_{eff}(t)$ tends to be monotonic for smaller vibration amplitude but nonmonotonic for larger vibration amplitude. In addition, the sample sees an accompanying radial field component (as div $\mathbf{B}=0$), which provides a transverse ac field perturbation. Together with the longitudinal and transverse field perturbations, possible tearing of the vortices from the pinning centers due to the sample vibration gives rise to a highly effective mechanism to suppress the irreversibility. It is a general observation that the increase in dH/dt enhances the irreversibility while the increase in vibration amplitude has the opposite effect of suppressing the irreversibility.[10] Reversible magnetization over the largest field range is obtained by a combination of the highest vibration amplitude and the lowest sweep rate.[10]

III. RESULTS

In Fig. 3(a), we show two hysteresis loops measured with $dH/dt=0.1$ T/min, but using two different vibration amplitudes (a) 0.12 and (b) 1.2 mm. The field is applied in a direction midway between [100] and [110] of the V_3Si crystal. We denote this orientation by ϕ_1. Both the curves exhibit a pronounced peak effect with the maximum hysteresis identifying the peak position H_p. Hysteresis is smaller over the entire field range in the latter case. But, there is a marked

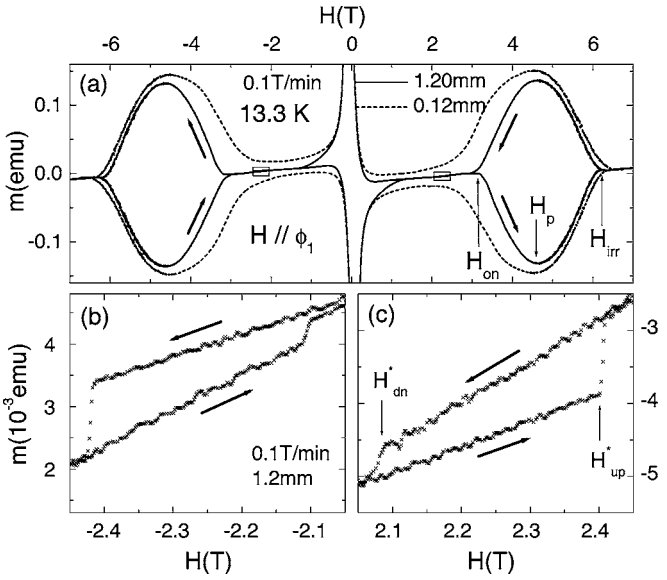

FIG. 3. (a) Four quadrant hysteresis loops at $dB/dt = 0.1$ T/min. Full line and dotted line correspond to 1.2 and 0.12 mm vibration amplitude, respectively. Magnetization in the field range $2T \leqslant |B| \leqslant 2.5T$ (the two boxes in the reversible regime) is magnified in (b) and (c). The arrows indicate the direction of the field scan. The peak position H_p, onset of the peak H_{on} and the irreversibility field H_{irr} are marked by arrows.

difference below the onset of the peak H_{on}, where the hysteresis begins to grow rapidly. While the magnetization obtained using 1.2 mm amplitude is reversible, that using 0.12 mm amplitude has a substantial hysteresis, which originates mainly from the metastable nonequilibrium disordered vortex phase. In case of (b) (1.2 mm), larger ac field perturbation due to the larger amplitude is adequate to eliminate or *anneal* the nonequilibrium disordered phase below the peak and make the magnetization reversible. As can be seen in Fig. 3(a), H_{on} is highly sensitive to the measurement parameters. The reversible or equilibrium magnetization is the focus of this paper.

The key result is presented in Figs. 3(b) and 3(c), where the field window $2T \leqslant |B| \leqslant 2.5T$ from the two boxes in Fig. 3(a) is magnified. The reversible magnetization (1.2 mm) shows an abrupt step at fields H^*_{up} and H^*_{dn} ($\leqslant H^*_{up}$) in the ascending and descending fields ($|B|$), respectively. Under optimal measuring conditions, width of the magnetization step is of the order of 100 Oe. This is reminiscent of the magnetization step observed at the second magnetization peak in BSCCO by Avraham *et al.*[9] But, the hysteretic occurrence and the location of the step feature well below the onset of the peak are in contrast to the observation in BSCCO. The location of the steps almost coincides with the onset of the peak measured with minimal annealing (0.12 mm amplitude). In this case, the equilibrium feature is perhaps overwhelmed by the metastable phases and no step feature is observed. In the field scans, generally, the magnetization step is observed to be larger at H^*_{up} compared to that at H^*_{dn}. The magnetization steps are robust as also evident from the field cooled (FC) and zero field cooled (ZFC) temperature scans shown in Fig. 4. The change in the magnetization

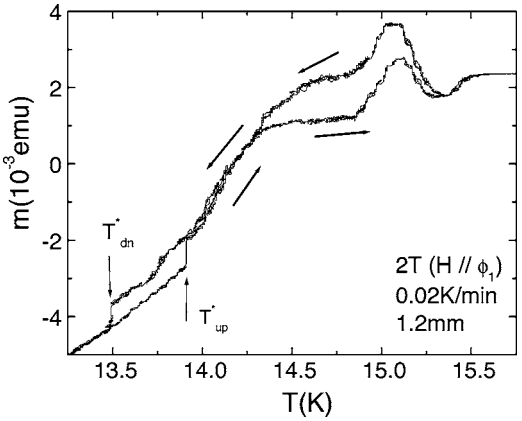

FIG. 4. M vs T at a field of 2 T. Arrows show the direction of temperature scan at the rate of 0.02 K/min. The hysteresis at higher temperatures is identified with the peak regime.

across the step (at H^*_{up} and T^*_{up}) is approximately 0.3 G. The occurrence of the magnetization steps is hysteretic in temperature scans as well, i.e., the step is at T^*_{up} in ZFC case and at T^*_{dn} in the FC case. The irreversibility in magnetization at further higher temperatures originates from the peak effect regime.

The step feature exhibits a weak dynamics. As shown in Fig. 5, gap between the two steps widens slightly as dH/dt is increased. Further, the step is sharper at smaller dH/dt. Similarly, the gap between the fields H^*_{up} and H^*_{dn} narrows with increasing amplitude (better annealing). We further note that the step feature is observed when both the parameters (dH/dt from 0.1 to 0.01 T/min and the amplitude of vibration from 1.2 to 0.3 mm) are simultaneously reduced (i.e., towards quasistatic limit). Below an amplitude of 0.3 mm, ac field perturbation is inadequate for dynamic equilibration and the magnetization becomes strongly irreversible and independent on further reducing the amplitude.

In Fig. 6, we discuss how the magnetization step evolves when dH/dt and the amplitude are independently varied. In Fig. 6(a), we show the ascending field curve for different values of dH/dt while the amplitude is held constant at 0.4

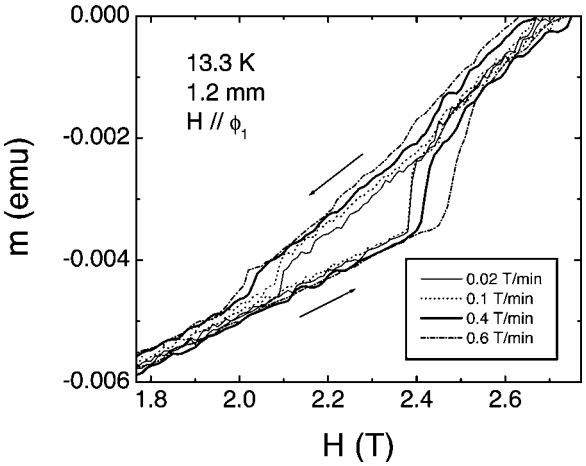

FIG. 5. The magnetization step feature at different field sweep rates. Vibration amplitude is kept constant at 1.2 mm.

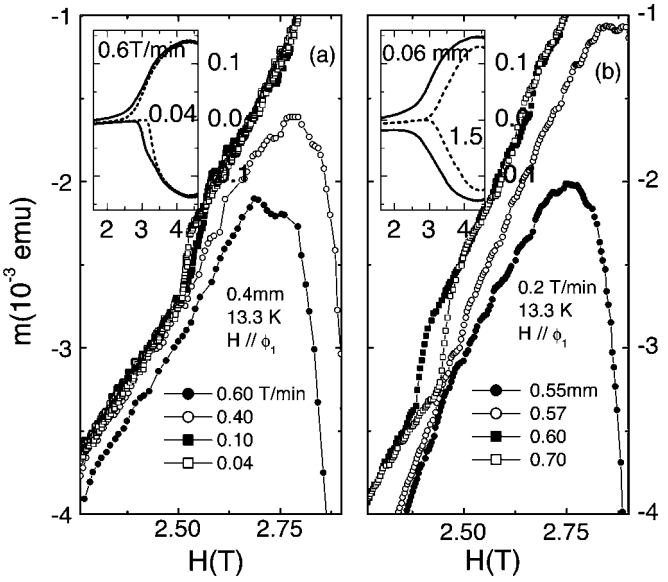

FIG. 6. Evolution of the magnetization step (a) for decreasing sweep rate (amplitude 0.4 mm). (b) Increasing amplitude (sweep rate 0.2 T/min).

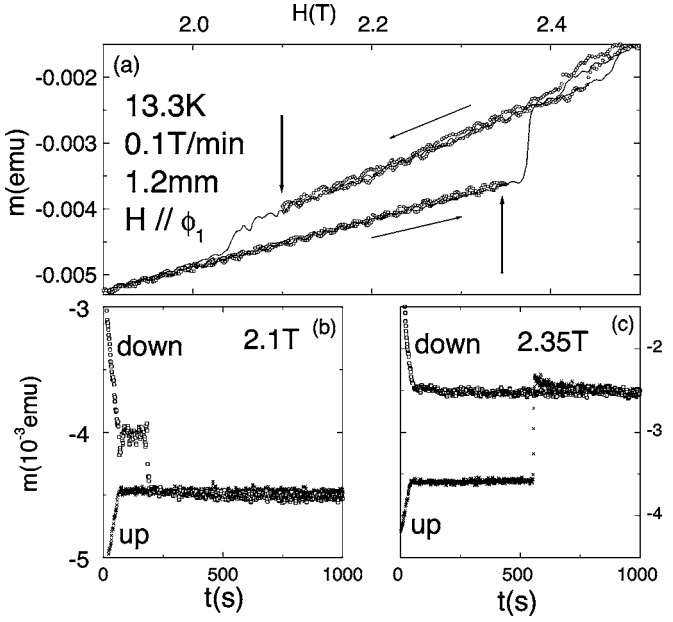

FIG. 7. (a) Figure 3(c) reproduced. Open circles are the magnetization obtained by a field excursion from below 2 T to a field less than H^*_{up}. Similar field excursion is carried out on the decreasing field branch. (b) Time relaxation of magnetization on the decreasing field branch at 2.1 T.

mm. As dH/dt is lowered, first a broad magnetization step appears, which evolves into a sharper step as dH/dt is further lowered. Conversely, in Fig. 6(b), we show the evolution of the magnetization step as the amplitude is increased while dH/dt is held fixed. Increasing the vibration amplitude and decreasing dH/dt are thus equivalent. We therefore conclude that the nonmonotonic field variation experienced by the sample is crucial for the equilibration process and the observation of the magnetization step.

As shown in Fig. 7(a), magnetization retraces on traversing the ascending (descending) field curve up and down as long as the maximum (minimum) field applied is kept below H^*_{up} (above H^*_{dn}). This result suggests that the magnetization is uniformly distributed (no bulk currents) and is constituted entirely by a surface current. We also measured the relaxation of magnetization at a field slightly below H^*_{up} (above H^*_{dn}) on the ascending (descending) field branch. Magnetization spontaneously jumps to the value on the descending (ascending) field branch after a waiting time t_{up} (t_{dn}) as shown in Figs. 7(b) and 7(c). We have repeated this experiment several times at each of these fields. This result suggests that there exist two distinct stable states. It is perhaps not possible to access any intermediate magnetization values between ascending and descending field curves by any combination of field excursions or relaxation procedures. Far from H^*_{up} and H^*_{dn}, no relaxation or jump is seen even after two hours. We note that t_{up} is usually much larger than t_{dn}.

In Fig. 8, we present the phase diagram of sample SA obtained from detailed measurements at different temperatures for the field orientation ϕ_1. Filled (open) circles are H^*_{up} (T^*_{up}) and H^*_{dn} (T^*_{dn}), obtained by isothermal field scans (temperature scans in constant field). Data obtained from field and temperature scans coincide in the H-T phase space. H^*_{up} and H^*_{dn} closely follow H_{on} and H_p in all the three samples studied. We also show the second critical field H_{c2} and irreversibility line H_{irr}. The region enclosed by the continuous line is reversible within the experimental resolution corresponding to J_c=5 A/cm^2. The annular region between the 5 A/cm^2 line and $H_{LF/HF}$ is characterized by pronounced history effects as measured by minor magnetization curves.[18] H_{LF} and H_{HF} denote the low-field and high-field order disorder transitions, respectively.[5] With decreasing temperature, lifetime of the metastable disordered phase becomes larger and the nonequilibrium phases cannot be annealed anymore. This effect limits observation down to temperatures of about 10 K. Below 13 K, it is not possible to eliminate the hysteresis below the H_{on} even under extreme annealing conditions possible in our experiment. But at higher temperatures the

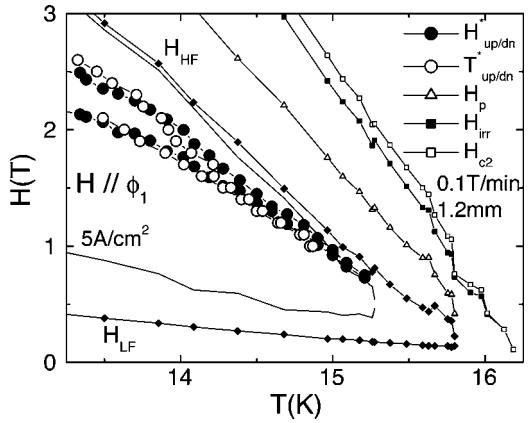

FIG. 8. Phase diagram showing $H^*_{up/dn}$ (filled circles), $T^*_{up/dn}$ (open circles), H_p (open triangles), H_{irr} (filled squares), and H_{c2} (open squares). The reversible region is enclosed by the line marked by 5 A/cm^2. The region beteen 5 A/cm^2 line and the $H_{LF/HF}$ (filled diamonds) is characterized by history effects.

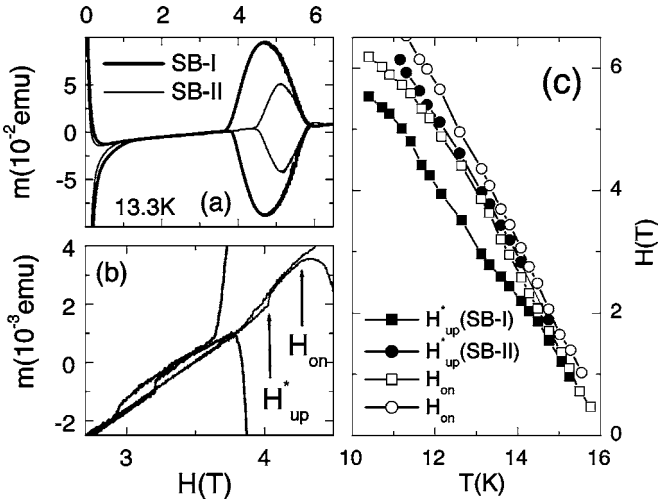

FIG. 9. (a) Magnetization hysteresis loops of samples SB-I (thick line) and SB-II (thin line). (b) Reversible part below the peak onset H_{on} is expanded to show the magnetization step feature. H^*_{up} and H_{on} are indicated. (c) Phase diagram of SB-I and SB-II. $H^*_{up}(T)$ (filled symbols) and $H_{on}(T)$ (open symbols). All these data are taken for an orientation close to ϕ_1.

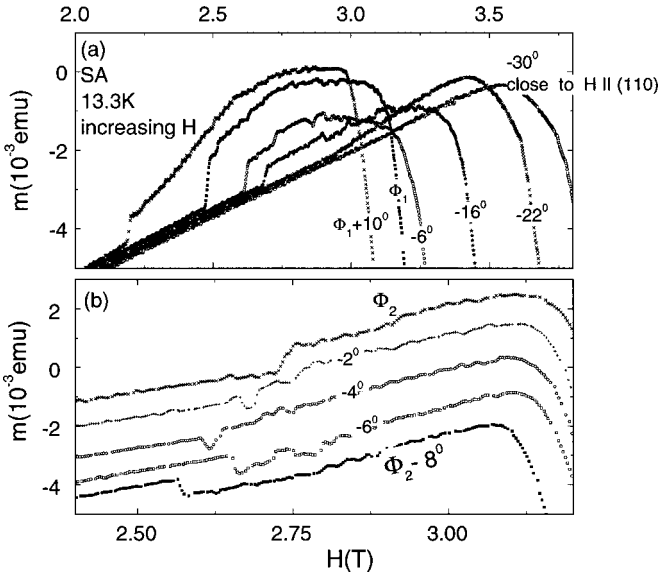

FIG. 10. (a) Reversible magnetization for the field oriented in different directions with respect to the crystal symmetry axes. All the data in previous figures are for the angle marked ϕ_1 corresponding to the field direction intermediately between [100] and [110]. The curve marked −30° is recorded with field applied very close to [110] direction. At this angle no step in $\mathbf{m}_{eq}$ has been observed. Similarly, no step is observed for orientations beyond ϕ_1+10°, which is very close to [100]. All these data are recorded for increasing field. (b) For different rotation axes, we have even observed the evolution of the positive step into a negative step when the orientation is changed by 8°.

gap between H^*_{up} (T^*_{up}) and H^*_{dn} (T^*_{dn}) tends to disappear. Beyond 15.2 K the low-field and high-field disordered phases begin to overlap and the reversible region disappears.

Two other spherical samples (SB-I and SB-II) with lower pinning strength compared to sample SA have also been found to be showing the step feature [see Figs. 9(a) and 9(b)]. BG-VG transition (peak effect) is governed by the field strength at which pinning interaction overcomes the intervortex interaction. Accordingly, decreasing pinning strength shifts the peak effect to higher fields. We also observe that, the onset and the peak are closely followed by the magnetization step feature with the same dependence on temperature and pinning strength as shown in Fig. 9. It is therefore tempting to associate the step feature with the order-disorder transition. Further, the difference between H^*_{up} and H^*_{dn} narrows with decrease in the pinning strength in addition to a decrease in the magnetization step itself. This is consistent with a similar result on the sample SA with increasing temperature, which is equivalent to a decrease in the pinning.

As discussed earlier, V_3Si exhibits a small anisotropy in H_{c2}. But, the behavior of the magnetization step feature for different field orientations with respect to the crystallographic symmetry axes is very surprising. As shown in Fig. 10(a), the magnetization step is the largest for the angle marked ϕ_1 (corresponding to the field direction midway between [100] and [110]). Moving towards [100] (ϕ_1+10° and beyond) and [110] directions (ϕ_1-30°), the step reduces and finally vanishes for field directions coinciding with either of the symmetry directions. This suggests that there is a correlation between the observed magnetization step and the underlying crystal structure. This is further investigated by studying the vector magnetization data presented below. For a different rotation axis the positive step at ϕ_2 evolves into a negative step at ϕ_2-8° [see Fig. 10(b)]. We further note that there is a structure in the reversible magnetization after the major step leading up to the onset of the peak.

We analyzed the relative orientation between the field and the reversible magnetic moment $\mathbf{m}_{eq}$ by measuring the magnetic moment parallel and perpendicular to the applied field (assumed to be along $\mathbf{z}$). $\mathbf{m}_{eq}$ is expected to be along $-\mathbf{z}$ for spherically shaped isotropic specimens. At low fields, where magnetization is hysteretic, the angle θ (see the inset of Fig. 11) between $\mathbf{m}_{eq}$ and $-\mathbf{z}$ is nearly zero (not shown). Similarly, above the onset of the peak, $\theta\approx 0^\circ$ and 180° for increasing and decreasing field branches, respectively [see Fig. 11(b)]. This can be understood from the fact that the vortex matter in both these regimes is a pinned liquid with no preferred orientation. On the contrary, in the Bragg glass regime where magnetization is reversible, $\mathbf{m}_{eq}$ is oriented away from the $-\mathbf{z}$ direction with angle θ between them in the range of 0°–20°. There is a tendency for the $\mathbf{m}_{eq}$ to orient towards one of the crystal symmetry directions. The value of θ in the BG regime is close to zero for field oriented along a symmetry direction. Coinciding with the magnetization step, $\mathbf{m}_{eq}$ in the increasing field cycle abruptly turns further away from the $-\mathbf{z}$ direction. We would like to mention here that the rotation is neither significant nor is it abrupt when the field is along [110] or [100] directions. The orientation of the $\mathbf{m}_{eq}$ is, however, restored in the decreasing field branch as shown in Fig. 11(b) in such a way that the θ vs H curves exhibit abrupt steps at the same fields as in the case of $\mathbf{m}_{eq}$ vs H curves. In other words, θ vs H curves too exhibit hysteresis. We further note that the reorientation is also observed to accompany the

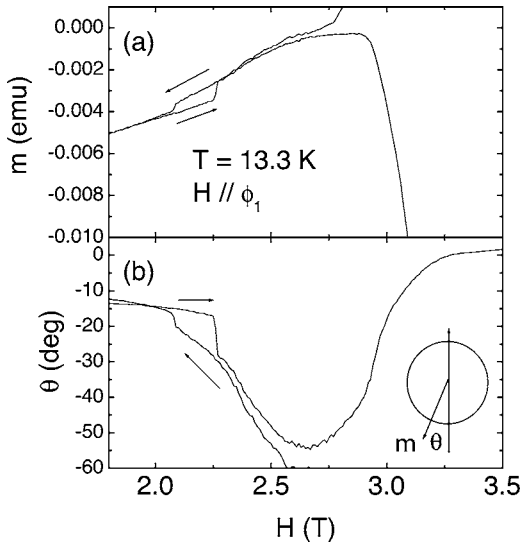

FIG. 11. (a) Magnetization step feature reproduced from Fig. 3 with part of the peak region shown on the right. (b) The angle θ between $\mathbf{m}_{eq}$ and the $-\mathbf{z}$ (see the inset) as a function of field in the increasing field branch. We note that $\theta \approx 0$ with the onset of hysteresis in the peak regime.

magnetization step in temperature sweeps. These general observations also apply to the samples SB-I and SB-II.

IV. DISCUSSION OF RESULTS

The dynamical equilibration process exploits the ac field ripple experienced by the sample during a measurement in VSM to produce a reversible magnetization ($J_c \leq 5$ A/cm^2) prior to the peak effect. Equilibrium magnetization exhibits an abrupt first-order-like step below the onset of the peak effect. Mean position of the steps in ascending and descending fields $(H^*_{up}+H^*_{dn})/2$ is robust under different dH/dt and sample vibration amplitude. The same is not the case with the onset field H_{on} and the extent of hysteresis $(H^*_{up}-H^*_{dn})/2$. The step feature may not be a manifestation of the BG-VG transition because, it depends crucially on the relative orientation between the crystallographic axis and the field. The step even vanishes for fields along the crystal symmetry directions although peak effect is observed for all orientations. Examination of the samples of different pinning strength revealed that the location of the magnetization step as well as the peak effect move to higher fields with decreasing pinning strength, very similar to the peak effect itself (Fig. 9). This suggests that any mechanism to explain the phenomenon should involve the pinning strength.

In the reversible regime, magnetization is predominantly due to surface current, which has two contributions. First, due to the equilibrium magnetization in the bulk, which is determined by the Gibbs free energy

$$G(H) = U_{el} - \mathbf{B} \cdot \mathbf{H}, \tag{1}$$

where U_{el} is the elastic interaction between the vortices, $\mathbf{B}$ the induction, and $\mathbf{H}$ the applied field. This contribution must be reversible. Secondly, boundary conditions dictate that the vortices must be perpendicular to their surface. But in the interior of the sphere, they should orient along the applied field so that $G(H)$ is minimized. The current associated with the vortex bending at the surface provides an additional contribution to the magnetic moment. For an ideal spherical surface, this contribution should also be reversible. We attribute the hysteresis observed around the magnetization steps to the roughness on the sample surface. The order of magnitude of the roughness is less than a micrometer.[19]

More intriguing result is the abrupt orientational change in the magnetization accompanying the magnetization step. We believe that the observed orientation change can account for the magnetization step. But the extent of the magnetization rotation translates into a tiny rotation of the FLL. To understand the orientational transition, we propose an additional term in the Gibbs free energy E_{an} to account for the coupling between the FLL and the crystal structure due to a possible order parameter anisotropy. Such a coupling does exist in V_3Si as evident from the experiments of Yethiraj *et al.*[12] E_{an} is similar to the magnetocrystalline anisotropy term in ferromagnets. Here, E_{an} is postulated to be minimum for the FLL oriented along a symmetry direction. It increases as the FLL turns away from the crystal symmetry direction. For instance, we write

$$G(H) = U_{el} - \mathbf{B} \cdot \mathbf{H} + E_{an}. \tag{2}$$

Let us consider the case of field H oriented along a symmetry direction. Both the second and third terms on the right-hand side of Eq. (2) automatically minimize the $G(H)$ provided $B \| H$. But for H oriented away from a symmetry direction, these two terms are in conflict with each other. The second term on the right favors FLL parallel to the applied field while the third term favors the FLL to be oriented along a symmetry direction. We believe that the orientational transition is a result of the competition between these two terms. But it is unreasonable to expect that the FLL is capable of abruptly tilting over the entire sample. The energy barrier offered by the surfaces for such a process would be insurmountable. In the discussion so far, the role of pinning is not considered explicitly. We imagine that the point pinning structure essentially breaks up the FLL into a large number of smaller domains. Individual domains, rather than the entire FLL, independently tilt across the transition and connect up with the rest of the lattice. For this to occur, the domains have to be small enough for this process to be energetically favorable, yet may be large enough that the magnetization is reversible within experimental resolution.

To summarize, this transition is the result of FLL-crystal lattice coupling, which we contend, cannot be observed in a macroscopic sample in the absence of pinning just as the peak effect can not be seen in an ideally pin free sample. Pinning breaks up the FLL into domains. We understand that, smaller the domain, it is easier to reorient. We know that at a given field below the peak effect, domains are expected to be larger for a sample of weaker pinning and reorientation is favorable at higher fields. As mentioned earlier, both the peak effect and the reorientation transition shift to higher fields in samples with weaker pinning. As seen in Fig. 10, there are several smaller steps following the major magneti-

zation step. We attribute this to local variation in pinning.

The reorientation transition may be first order in nature. A second-order transition in the FLL in the bulk confined by surface roughness potential may also account for the observed hysteresis. Thermal measurements are necessary to answer this question while small angle neutron scattering or μSR studies are necessary to understand the structural aspects of this transition.

V. CONCLUSIONS

Equilibrium magnetization is measured on spherical samples of V_3Si of different pinning strength exhibiting peak effect. In the field regime prior to the onset of the peak effect, irreversibility is eliminated by dynamic equilibration process by appropriately choosing the magnetic field sweep rate and the sample vibration amplitude in a vibrating sample magnetometer. This process exploits the small inhomogeneity in the external magnetic field, which effectively provides a tiny oscillatory field on the sample. The reversible magnetization exhibits a small "first-order-like" step with a prominent hysteresis in field and temperature scans provided the field is orientated away from [110] and [100] directions. Accompanying the magnetization step is a reorientation of the magnetization. Study of samples of differing pinning strength reveals that the magnetization step closely follows the onset field of peak effect. We suggest a coupling between the flux line lattice and the crystal lattice to play a role in the FLL reorientation.

ACKNOWLEDGMENTS

G.R. gratefully acknowledges the Alexander von Humboldt Foundation for their financial support during his visit of the Institut fur Festkorperphysik (IFP), Forschungszentrum Karlsruhe, Germany. He is also grateful to IFP for the travel support. The authors thank Professor S. Bhattacharya for discussion.

[1] T. Giamarchi and P. Le Doussal, Phys. Rev. Lett. **72**, 1530 (1994); Phys. Rev. B **52**, 1242 (1995).

[2] M. J. Higgins and S. Bhattacharya, Physica C **257**, 232 (1996).

[3] B. Khaykovich, M. Konczykowski, E. Zeldov, R. A. Doyle, D. Majer, P. H. Kes, and T. W. Li, Phys. Rev. B **56**, R517 (1997).

[4] Y. Paltiel, E. Zeldov, Y. Myasoedov, H. Shtrikman, S. Bhattacharya, M. J. Higgins, Z. L. Xiao, E. Y. Andrei, P. L. Gammel, and D. J. Bishop, Nature (London) **403**, 398 (2000).

[5] G. Ravikumar, H. Küpfer, A. Will, R. Meier-Hirmer, and Th. Wolf, Phys. Rev. B **65**, 094507 (2002).

[6] G. Ravikumar, V. C. Sahni, A. K. Grover, S. Ramakrishnan, P. L. Gammel, D. J. Bishop, E. Bucher, M. J. Higgins, and S. Bhattacharya, Phys. Rev. B **63**, 024505 (2001).

[7] T. Nishizaki *et al.* (unpublished).

[8] M. Willemin, C. Rossel, J. Hofer, H. Keller, A. Erb, and E. Walker, Phys. Rev. B **58**, R5940 (1998); M. Willemin, A. Schilling, H. Keller, C. Rossel, J. Hofer, U. Welp, W. K. Kwok, R. J. Olsson, and G. W. Crabtree, Phys. Rev. Lett. **81**, 4236 (1998).

[9] N. Avraham, B. Khaykovich, Y. Myasoedov, M. Rappaport, H. Shtrikman, D. E. Feldman, T. Tamegai, P. H. Kes, M. Li, M. Konczykowski, K. van der Beek, and E. Zeldov, Nature (London) **411**, 451 (2001).

[10] H. Küpfer, G. Ravikumar, Th. Wolf, A. A. Zhukov, and R. Meier-Hirmer, Phys. Rev. B **70**, 144509 (2004).

[11] M. R. Eskildsen, P. L. Gammel, B. P. Barber, U. Yaron, A. P. Ramirez, D. A. Huse, D. J. Bishop, C. Bolle, C. M. Lieber, S. Oxx, S. Sridhar, N. H. Andersen, K. Mortensen, and P. C. Canfield, Phys. Rev. Lett. **78**, 1968 (1997); Y. De Wilde, M. Iavarone, U. Welp, V. Metlushko, A. E. Koshelev, I. Aranson, G. W. Crabtree, and P. C. Canfield, *ibid.* **78**, 4273 (1997).

[12] M. Yethiraj, D. K. Christen, D. McK. Paul, P. Miranovic, and J. R. Thompson, Phys. Rev. Lett. **82**, 5112 (1999).

[13] V. G. Kogan, P. Miranovic, Lj. Dobrosavljevic-Grujic, W. E. Pickett, and D. K. Christen, Phys. Rev. Lett. **79**, 741 (1997).

[14] R. Meier-Hirmer, H. Küpfer, and H. Scheurer, Phys. Rev. B **31**, 183 (1985).

[15] B. W. Battermann and C. S. Barrett, Phys. Rev. **145**, 296 (1966).

[16] H. Küpfer, G. Linker, G. Ravikumar, Th. Wolf, A. Will, A. A. Zhukov, R. Meier-Hirmer, B. Obst, and H. Wühl, Phys. Rev. B **67**, 064507 (2003).

[17] The field inhomogeneity in the magnet can be well described by $\Delta H \approx H(0) \times 2.5 \times 10^{-3} z^2$ (z in cm). Actual axial field component experienced by the sample tends to be monotonic in time when $dH/dt \geq 2n\Delta H$ where n is the frequency of sample vibration (=45 Hz). We note that always a strong annealing is achieved when $dH/dt \leq 2n\Delta H$. The transverse field perturbation is estimated to be also of the same magnitude as ΔH. Further, the magnitude of the field perturbation is proportional to the amplitude A and $H(t)$ and therefore annealing of the irreversibility is much more effective at a lower dH/dt, higher H and higher A.

[18] G. Ravikumar, P. K. Mishra, V. C. Sahni, S. S. Banerjee, A. K. Grover, S. Ramakrishnan, P. L. Gammel, D. J. Bishop, E. Bucher, M. J. Higgins, and S. Bhattacharya, Phys. Rev. B **61**, 12490 (2000); S. B. Roy and P. Chaddah, J. Phys.: Condens. Matter **9**, L625 (1997); G. Ravikumar, K. V. Bhagwat, V. C. Sahni, A. K. Grover, S. Ramakrishnan, and S. Bhattacharya, Phys. Rev. B **61**, R6479 (2000); S. Kokkaliaris, P. A. J. de Groot, S. N. Gordeev, A. A. Zhukov, R. Gagnon, and L. Taillefer, Phys. Rev. Lett. **82**, 5116 (1999).

[19] Some of the experiments on a sample of the same pinning strength as sample SA but of a cuboid geometry did not yield the magnetization step although magnetization is reversible below the peak field. The sharp edges of the cuboid geometry may perhaps block the FLL from reorienting towards a crystal symmetry direction.